Journal of Magnetism and Magnetic Materials 321 (2009) 1092–1099

Contents lists available at ScienceDirect

Journal of Magnetism and Magnetic Materials

journal homepage: www.elsevier.com/locate/jmmm

Impact of zinc substitution on the structural and magnetic properties of chemically derived nanosized manganese zinc mixed ferrites

E. Veena Gopalan [a], I.A. Al-Omari [b], K.A. Malini [c], P.A. Joy [d], D. Sakthi Kumar [e], Yasuhiko Yoshida [e], M.R. Anantharaman [a,*]

[a] Department of Physics, Cochin University of Science and Technology, Cochin 682 022, Kerala, India
[b] Department of Physics, College of Sciences, Sultan Qaboos University, PO Box 36, Postal Code 123, Muscat, Sultanate of Oman
[c] Department of Physics, Vimala College, Thrissur 680 009, Kerala, India
[d] National Chemical Laboratory, Physical Chemistry Division, Pune 411 008, India
[e] Department of Applied Chemistry, Bio-Nano Electronics Research Centre, Toyo University, Kawagoe, Saitama 350-8585, Japan

ARTICLE INFO

Article history:
Received 25 July 2008
Received in revised form
9 October 2008
Available online 11 November 2008

Keywords:
Manganese zinc ferrite

ABSTRACT

$Mn_{1-x}Zn_xFe_2O_4$ nanoparticles ($x = 0$–1) were synthesized by wet chemical co-precipitation techniques. X-ray diffraction, transmission electron microscopy and high-resolution transmission electron microscopy were effectively utilized to investigate the different structural parameters. The elemental analysis was conducted using energy-dispersive spectrum and inductively coupled plasma analysis. The magnetic properties such as magnetization and coercivity were measured using vibrating sample magnetometer. The observed magnetization values of the nanoparticles were found to be lower compared to the bulk counterpart. The magnetization showed a gradual decrease with zinc substitution except for a small increase from $x = 0.2$ to 0.3. The Curie temperature was found to be enhanced in the case of ferrites in the nanoregime. The variation in lattice constant, reduced magnetization values, variation of magnetization with zinc substitution, the presence of a net magnetic moment for the zinc ferrite and the enhancement in Curie temperature in $Mn_{1-x}Zn_xFe_2O_4$ all provide evidence to the existence of a metastable cation distribution together with possible surface effects at the nanoregime.

1. Introduction

Nanosized manganese ferrite is found to be exhibiting interesting structural and magnetic properties. The possible applications of manganese ferrite nanoparticles are in magnetic storage, as precursors for ferrofluids, as contrast enhancing agents in magnetic resonance imaging (MRI), as magnetic refrigerant materials in magnetic refrigeration technology and magnetically guided drug-delivery agents [1,2].

Manganese ferrites belong to the class of spinel ferrites. The equilibrium distribution of cations in the bulk structure is influenced by a number of factors namely ionic radii, ionic charge, lattice energy, octahedral site preference energy and crystal field stabilization energy. For example, in the coarser regime, Zn^{2+} has a strong preference for tetrahedral sites while Ni^{2+} exhibits a strong octahedral preference in spinel ferrites. Cations like Mn^{2+}/Mn^{3+} are found to be influencing the magnetic, structural and electrical properties considerably. In the nanoregime, in case of spinel ferrites, there are distinct deviations in magnetic properties with respect to their bulk counterparts. For instance, though zinc ferrite is a normal spinel in the micron regime and non-magnetic, in the nanoregime it is found to exhibit an inversion and hence exhibit a net magnetization at room temperature [3–5]. Nanosized nickel ferrite is reported to be exhibiting increased magnetization by some researchers [6], while others have reported reduced magnetization with respect to their bulk counterparts [7]. The core shell models have been invoked to account for the reduced magnetization of nano-nickel ferrite while cation redistribution and the existence of surface spins have been attributed to the case where there is increased magnetization.

However, the role of cations vis-a-vis their occupancy of octahedral sites instead of tetrahedral sites is still not clear as regards their influence in deciding the overall magnetic properties of these materials in the nanoregime. It is in this context that a study of nanosized $MnFe_2O_4$ with varying concentration of zinc assumes significance. Ferrites belonging to the series $Mn_{1-x}Zn_xFe_2O_4$ (for $x = 0, 0.1, 0.2, \ldots, 1$) provides an ideal platform to check various hypotheses. Moreover the role of Jahn–Teller ions like Mn^{3+}/Mn^{4+} can also be investigated in influencing the overall magnetic properties of mixed ferrites.

When ascertaining the role of cations, the knowledge of exact stiochiometry is important in the case of mixed ferrites belonging

* Corresponding author. Tel.: +91 4842577404.
E-mail address: mraiyer@gmail.com (M.R. Anantharaman).

0304-8853/$ - see front matter © 2008 Elsevier B.V. All rights reserved.
doi:10.1016/j.jmmm.2008.10.031

to a series of this type. The exact and prior determinations of various ions in the compositions also provide valuable inputs in ascertaining the distribution of cation between sites. So compositional analysis using techniques like ICP/energy-dispersive X-ray spectra (EDS) enables one to determine the exact composition of the synthesized series. This will enable to determine deviations from expected stiochiometry and is vital in arriving at the exact cation distribution in the case of nanosized manganese zinc ferrites. Many researchers have ignored this aspect and their conclusions are often misleading and erroneous, especially, if cation distribution is the deciding factor in determining the overall magnetic properties of the materials in the nanoregime.

In the bulk, $MnFe_2O_4$ is found to be 20% inverse with a stoichiometry of $Mn_{0.8}Fe_{0.2}[Mn_{0.2}Fe_{0.8}]O_4$ where cations in brackets occupy octahedral sites [8]. A higher inversion up to 60% has been reported in nanosized manganese ferrite [9]. When zinc is substituted for manganese in $Mn_{1-x}Zn_xFe_2O_4$, the zinc ions are expected to occupy the tetrahedral sites. In ceramic samples the zinc ions were found to exist only in the tetrahedral sites (A sites) as expected. However, zinc is found to occupy octahedral sites in the case of nanosized manganese zinc ferrites when they are prepared by co-precipitation methods, or the pulsed laser deposition method or the high-energy ball-milling method [10]. The occupancy of zinc ions in octahedral sites in the nanoregime can alter the expected cation distribution to a great extent and will result in modified structural and magnetic properties in the case of $Mn_{1-x}Zn_xFe_2O_4$ nanoparticles.

2. Experimental

2.1. Synthesis of $Mn_{1-x}Zn_xFe_2O_4$ nanoparticles

Mixed ferrites belonging to the series $Mn_{1-x}Zn_xFe_2O_4$ ($x = 0$–1) nanoparticles were synthesized by wet chemical co-precipitation. Aqueous solutions of $(1-x)$ M manganese chloride ($MnCl_2 \cdot 4H_2O$), x M (x is the molar concentration of zinc) zinc chloride ($ZnCl_2$ anhydrous) and 2 M solution of ferric chloride ($FeCl_3$ anhydrous) were mixed to form a solution. This mixture solution was poured quickly into boiling 10 M NaOH solution diluted in 1800 ml of water under vigorous stirring. The formation of precipitate was found to be in the pH range, of 12.5–13. The solution was kept at 90 °C for 40 min under vigorous stirring. The precipitate was washed several times with distilled water, then filtered and dried in oven.

2.2. Characterization

X-ray diffraction (XRD) patterns of the samples were recorded using an X-ray powder diffractometer (Rigaku Dmax-C) using Cu-Kα radiation ($\lambda = 1.5405$ Å). Lattice parameter was calculated assuming cubic symmetry. The average crystallite size was estimated by using Debye Scherer's formula. The particle size was determined by subjecting the samples to transmission electron microscopy (TEM) (Joel JEM-2200 FS). High-resolution TEM (HRTEM) images, EDS and electron diffraction patterns were also obtained. Thermo Electron Corporation, IRIS INTRPID II XSP model was used for ICP measurement. Hysteresis loop parameters at room temperature and low temperature were evaluated by using a vibrating sample magnetometer. (DMS 1660 VSM) with external field varying from 13.5 to −13.5 kOe.

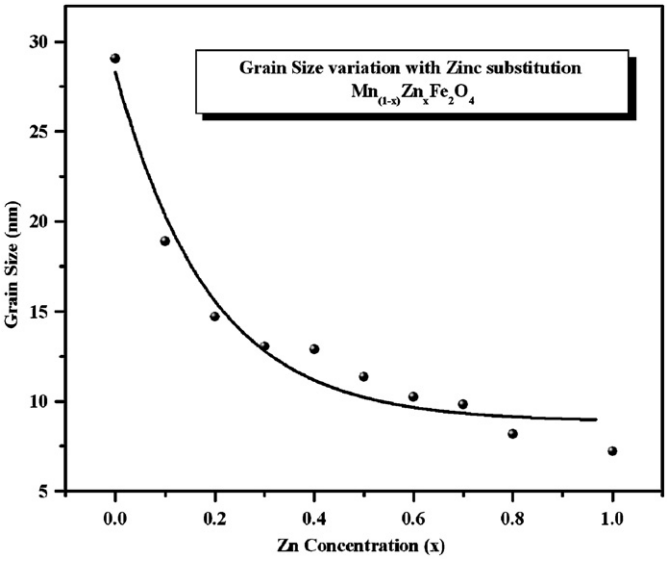

Fig. 2. Variation of grain size with zinc concentration.

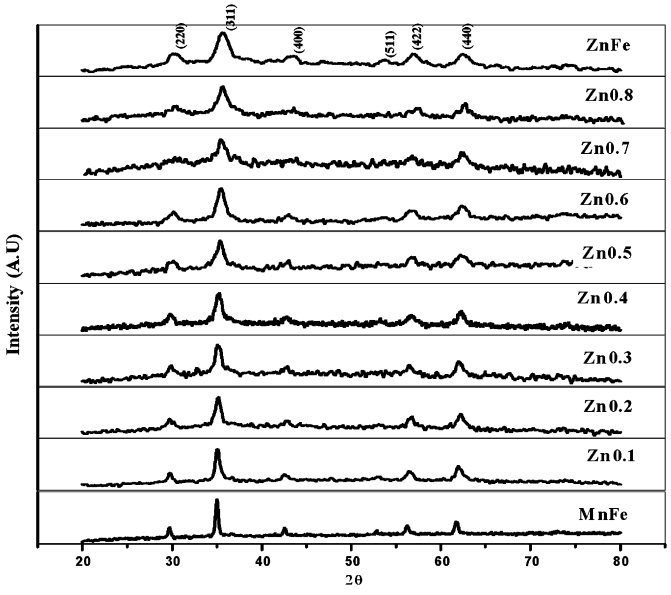

Fig. 1. XRD patterns of the series $Mn_{1-x}Zn_xFe_2O_4$ for different Zn substitution (x).

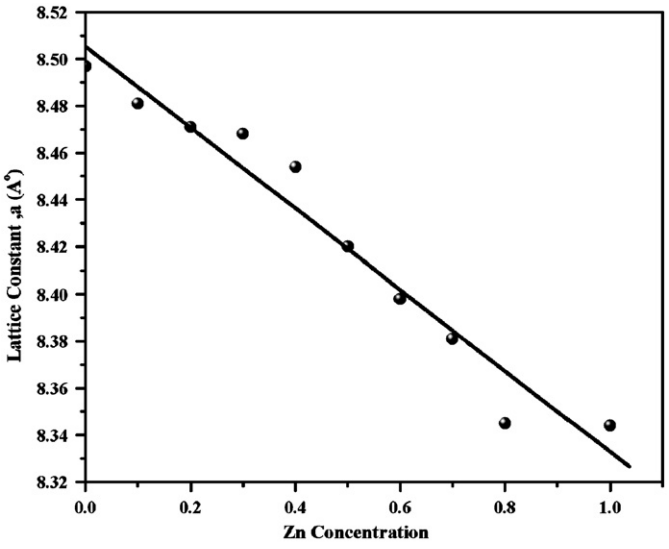

Fig. 3. Variation of lattice constant with zinc concentration.

3. Results and discussions

3.1. X-ray diffraction analysis

The XRD patterns of all the compounds belonging to the series $Mn_{1-x}Zn_xFe_2O_4$ (for $x = 0$–1) are shown in Fig. 1. The patterns are characteristic of an inverse spinel structure without any traces of detectable impurity. The size of the particles as evaluated by Debye Scherer's equation lies within the range 7–29 nm.

Further the variation of particle size with zinc substitution (x) was analysed and it is depicted in Fig. 2. It can be seen that for small amounts of zinc incorporation there is a sharp and significant decrease in particle size while for higher concentration of zinc, the decrease in particle size is less pronounced. It may be noteworthy that Arulmurugan et al. [11] noticed a linear trend in the variation of particle size and lattice parameter of nanosized $Mn_{1-x}Zn_xFe_2O_4$ mixed ferrites. It is to be construed here that an increase in zinc concentration in the solution during synthesis increases the reaction rate which favours the formation of ultrafine particles of mixed ferrites. The difference in average particle size between the extremes (for $x = 0$ and 1) was found to be approximately 20 nm which is quite significant. This accounts for the role of zinc substitution in reducing the particle size of the series.

The lattice parameter of all the compositions in the series of $Mn_{1-x}Zn_xFe_2O_4$ mixed ferrites was evaluated after assuming cubic symmetry. The variation of lattice parameter with zinc concentration is depicted in Fig. 3. A similar type of variation is also

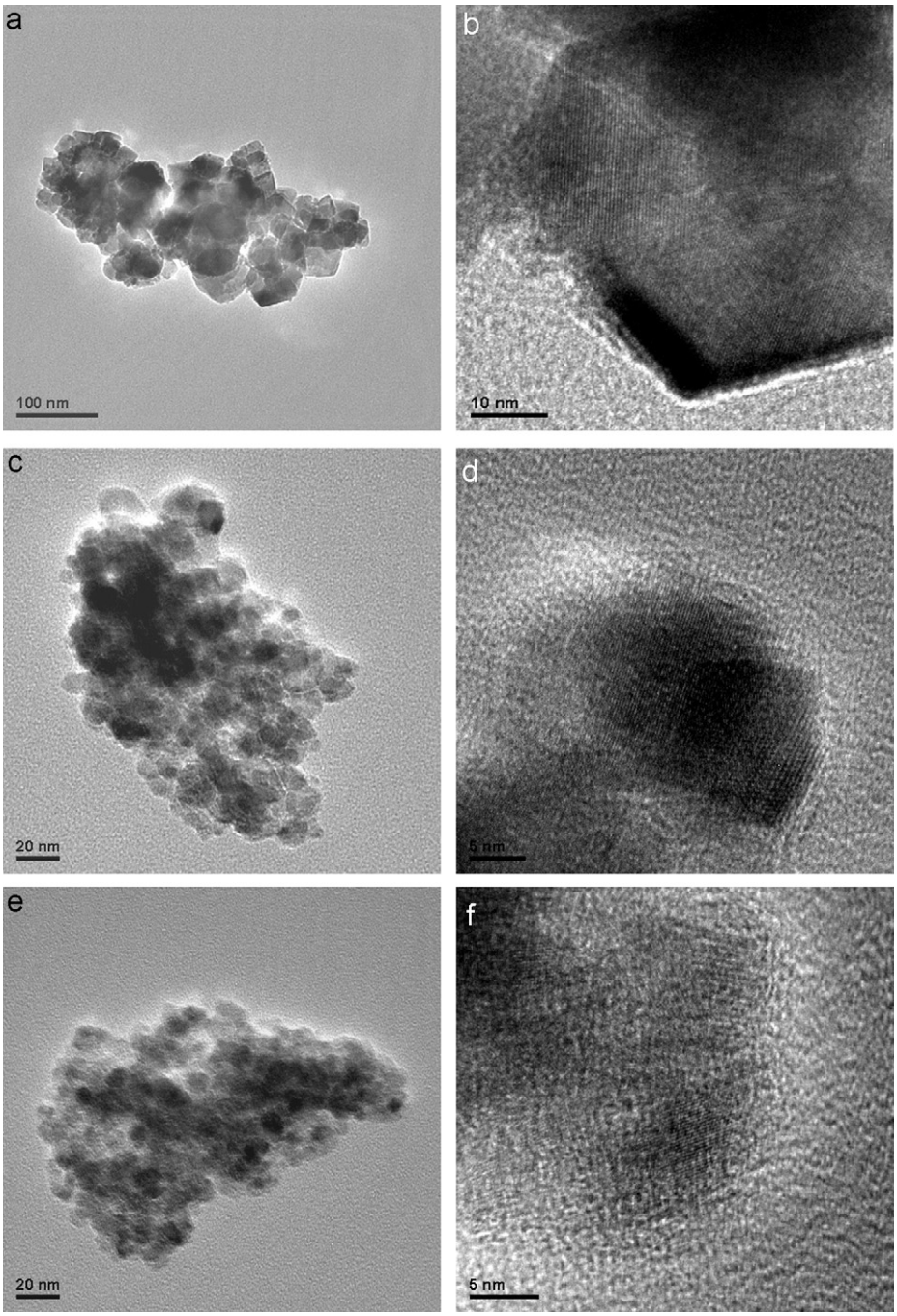

Fig. 4. TEM and HRTEM images of $MnFe_2O_4$ (a and b), $Mn_{0.5}Zn_{0.5}Fe_2O_4$ (c and d) and $ZnFe_2O_4$ (e and f).

observed in bulk $Mn_{1-x}Zn_xFe_2O_4$ which is attributed to the substitution of bigger sized Mn^{2+} cations (0.091 nm) by Zn^{2+} cations having a smaller radii (0.082 nm). However, a relative contraction of the lattice is observed with respect to bulk for the same composition (x) [12].

In the case of $Mn_{1-x}Zn_xFe_2O_4$ in the bulk form the presence of Mn^{2+}/Mn^{3+} ions and the volatilization of zinc were believed to be contributing to the contraction of the lattice [13]. However, chances of zinc evaporation are virtually nil since the methods adopted for the synthesis are based on cold co-precipitation techniques. But the chances for the formation of Mn^{3+} cations during the precipitation process cannot be ruled out since Mn^{2+} is easily oxidized in a highly basic solution [14]. Since Mn^{3+} ions have a preferential occupancy for octahedral geometry, they may be accommodated in the B site. In the process, in order to maintain charge neutrality of the B site, some Fe^{3+} ions may be converted into Fe^{2+} ions. The presence of Mn^{3+} and Fe^{2+} in octahedral site can result in the Jahn–Teller distortion of the octahedral symmetry of B sites which might lead to a lattice distortion in these mixed ferrites. This type of lattice distortion was observed in co-precipitated manganese ferrite nanoparticles [14].

3.2. Transmission electron microscopy analysis

HRTEM was employed to confirm the findings arrived through XRD studies. (Fig. 4a–f). TEM images of $MnFe_2O_4$ (Fig. 4a) particles exhibited truncated cubo-octahedral shapes along with spherical particles while the other two samples formed only spherical nanoparticles. The reduction in particle size with zinc concentration is evident in the TEM images. The HRTEM images of the three compositions have lattice spacings which confirm the crystalline nature of the sample. The particle sizes determined from TEM were found to be in agreement with that obtained from XRD studies. The electron diffraction pattern of $MnFe_2O_4$ and $ZnFe_2O_4$ particles are depicted in Fig. 5a and b respectively.

3.3. Compositional analysis using energy-dispersive X-ray spectroscopy and inductively coupled plasma analysis

Elemental analysis employing EDS and ICP is carried out on these compositions (Fig. 6). The compositions as determined by both EDS and ICP are compared and they are shown in Table 1. The ICP analysis of representative samples was carried out for the samples whose EDS have been measured. The estimated stoichiometry is shown in Table 1. It can be seen that the stiochiometry is very close to the anticipated values.

3.4. Magnetic characterization

Hysteresis loop parameters namely specific magnetization and coercivity were evaluated. They are tabulated and shown in Table 2. Representative loops are shown in Fig. 7 (300 K) and Fig. 8 (100 K).

The nanoparticles of the series $Mn_{1-x}Zn_xFe_2O_4$ were found to be showing reduced magnetization compared to their corresponding bulk counterparts [15]. The respective reduction in magnetization with respect to their bulk counterparts can be due to a rearrangement of cations because of the changed preferential occupancy in the case of nanosized ferrites, that is a change in distribution of Mn^{2+} and Zn^{2+} on the two sites.

The maximum magnetization value is showing a general decreasing trend except for an increase at $x = 0.2$–0.4 (Fig. 9). With increasing zinc incorporation the coercivity is showing a continuous decrease (Fig. 10). It is worth mentioning that zinc

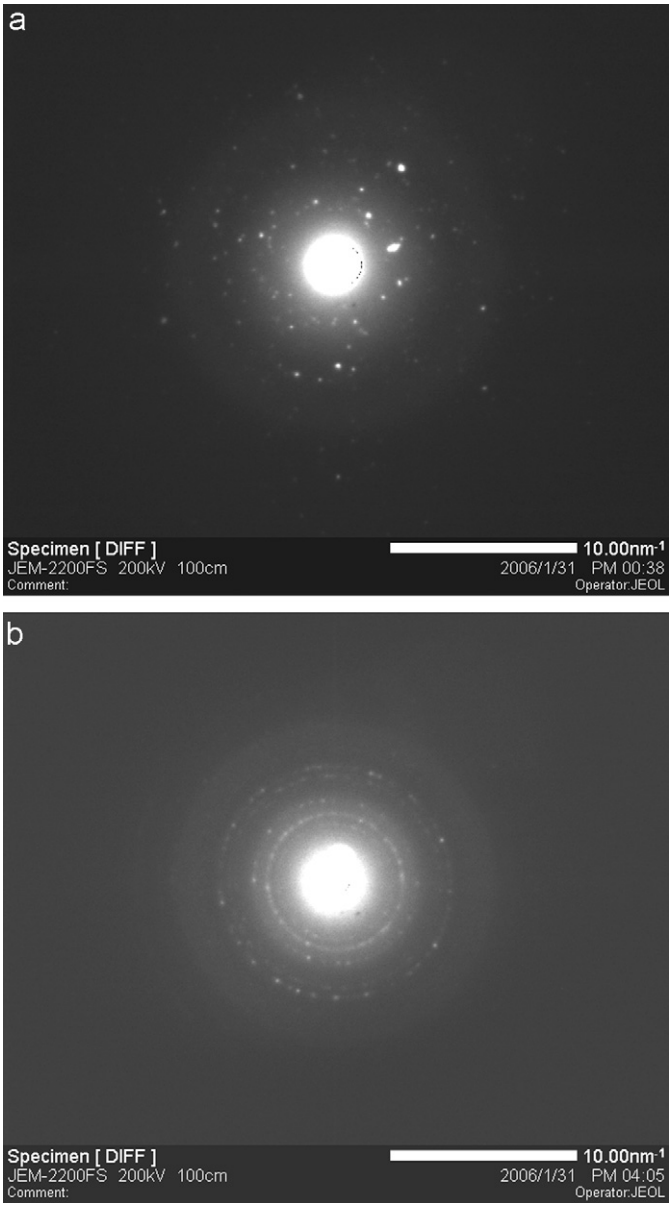

Fig. 5. Diffraction patterns of (a) $MnFe_2O_4$ and (b) $ZnFe_2O_4$ nanoparticles.

ferrite is found to possess magnetization value of 5.2 emu/g which is in agreement with the findings of various researchers [4,5].

In the case of $Mn_{1-x}Zn_xFe_2O_4$ prepared by standard ceramic techniques, the saturation magnetization value is found to increase with zinc substitution up to $x = 0.5$ and for further increase a decrease is obtained. This variation was qualitatively explained by the assumption that as the zinc content increases the relative number of ferric ions on the A sites diminishes and this reduces the A–B interaction [16].

The variation of maximum magnetization values with zinc concentration (Fig. 9) in the co-precipitated $Mn_{1-x}Zn_xFe_2O_4$ was found to deviate from the corresponding variation in bulk [15]. The lower magnitudes of magnetization and the occurrence of a net magnetic moment of the order of 5 emu/g in zinc ferrite (for $x = 1$) at room temperature is indicative of the presence of Zn^{2+} ions on the octahedral sites. The presence of Mn^{3+} ions together with its preference for octahedral sites can also result in a remarkable change in the cation distribution. The magnetic moments of $Mn^{2+}/Fe^{3+}$and Mn^{3+}/Fe^{2+} ions are 5 and 4 μ_B,

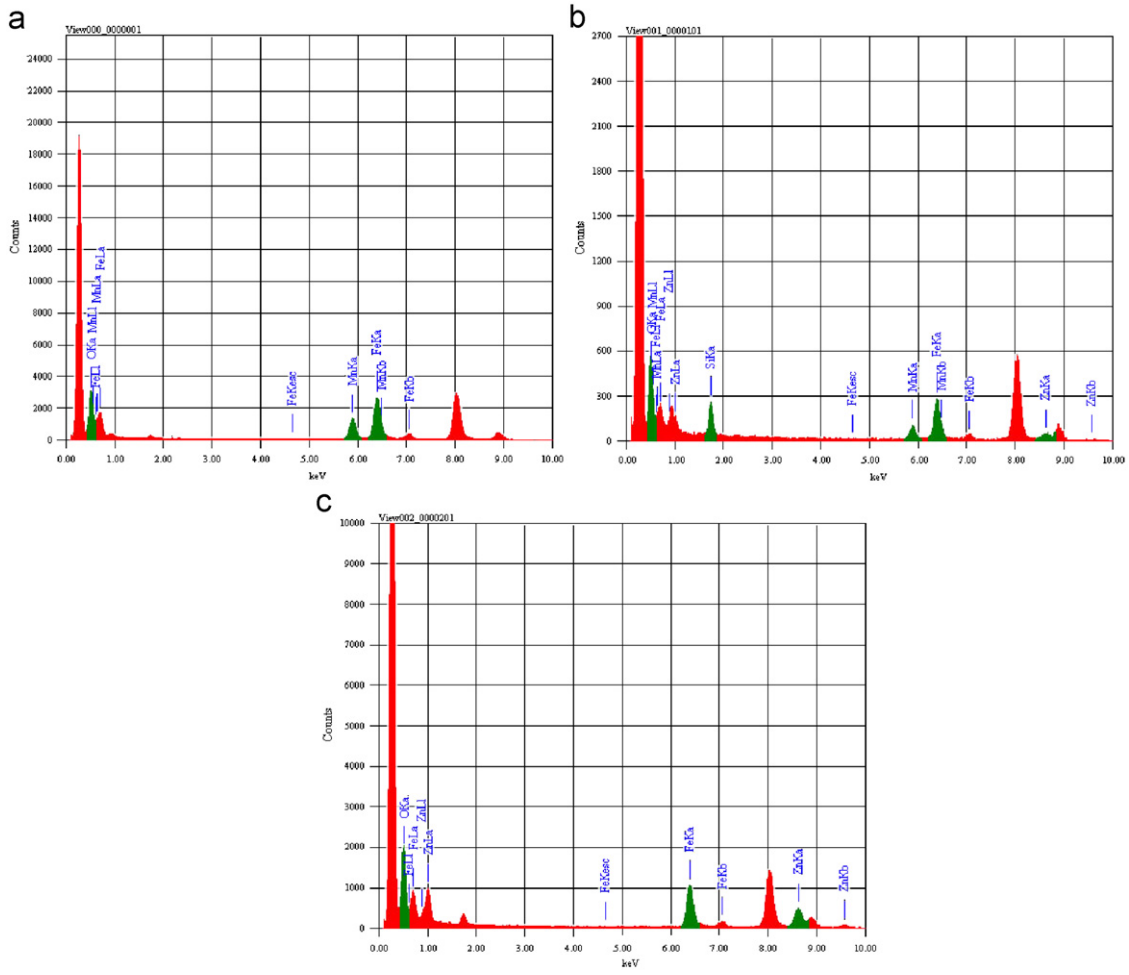

Fig. 6. EDAX spectrum of: (a) $MnFe_2O_4$, (b) $Mn_{0.4}Zn_{0.6}Fe_2O_4$ and (c) $ZnFe_2O_4$.

Table 1
Estimated stiochiometry from EDAX and ICP measurements.

Sample	Molar ratio	Expected	EDS	ICP
$MnFe_2O_4$	Mn:Fe	0.5	0.496	0.491
$Mn_{0.4}Zn_{0.6}Fe_2O_4$	Mn:Fe	0.2	0.189	0.191
	Zn:Fe	0.3	0.276	0.281
$ZnFe_2O_4$	Zn:Fe	0.5	0.465	0.468

respectively. Hence the presence of Mn^{3+}/Fe^{2+} pairs in the B lattice reduces the net magnetic moment of the octahedral lattice. This will create a decline in the net magnetization. Also the Jahn–Teller distortion was found to affect the magnetic properties in manganese containing ferrite [16]. The existence of random canting of particle surface spins, surface effects and the occurrence of a glassy state were reported to be playing an active role in the decline of magnetization values [17,18].

The temperature dependence of magnetization (M vs. temperature) is depicted in Fig. 11. The Curie temperature (T_c) was estimated by extrapolating the linear section of the temperature dependence of magnetization to the temperature axis. The T_c values of the nanoparticles were found to be larger than that observed for their bulk counterparts. This type of enhancement in T_c was observed in a number of nanoparticles of ferrites [19].

A reduction rather than an increase in T_c is expected in finite size systems based on theoretical grounds [20]. Hence the increase in T_c can be mainly attributed to the non-equilibrium cation redistribution as reported by Kulkarni et al. [10] in ultrafine $MnFe_2O_4$ particles. Higher degree of inversion was found to be associated with higher T_c values in ultra fine ferrite systems. The surface effect should also be considered while discussing the increase in T_c in nanoparticles. For smaller particles, a significant fraction of atoms is on the surface and hence a different type of interaction can be expected leading to a different average T_c.

The M–T curves of two samples $x = 0.5$ and 0.6 are exhibiting a cusp like behaviour before approaching zero magnetization or T_c. This cusp is absent for all compositions below $x = 0.5$. A similar cusp has been reported by Gajbhiye et al. [21] in $NiFe_2O_4$ nanoparticles. Wolski et al. [22] also attributed the cusp they observed in nanoparticles of $MnFe_2O_4$ to the transformation of one ferrimagnetic phase to another. Rath et al. [23] reported similar cusp like behaviour in Mn-rich compositions of the $Mn_{1-x}Zn_xFe_2O_4$ series and explained it as a result of a phase transition occurring at this temperature. The appearance of cusp in the case of $Mn_{0.5}Zn_{0.5}Fe_2O_4$ and $Mn_{0.4}Zn_{0.6}Fe_2O_4$ arises out of a transition from a metastable state to a stable state which is a result of the reorganization of cations between A and B sites.

With zinc substitution there is a general decrease in T_c values similar to bulk $Mn_{1-x}Zn_xFe_2O_4$ series (Fig. 12). This can be mainly attributed to weakened A–B exchange interaction which directly

Table 2
Structural and magnetic characteristic values of $Mn_{1-x}Zn_xFe_2O_4$.

$Mn_{1-x}Zn_xFe_2O_4$ (x)	Particle size (nm)	Lattice parameter (Å)	M (emu/g) $T = 300$ K	M (emu/g) $T = 100$ K	H_c (Oe) $T = 300$ K	H_c (Oe) $T = 100$ K	T_c °C	n_B (μ_B)
0	29.1	8.497	57	79	47	112	525	3.67
0.1	18.9	8.487	56	78	14	74	510	3.71
0.2	14.7	8.471	56	86	9	20	490	4.23
0.3	13.1	8.468	58	89	7	12	485	4.39
0.4	12.9	8.454	53	89	8	10	435	4.5
0.5	11.4	8.420	35	78	8	9	275, 480	4.26
0.6	10.3	8.398	31	75	8	9	255, 430	4.01
0.8	8.2	8.354	7.5		0			
1	7.2	8.414	5.2		0			

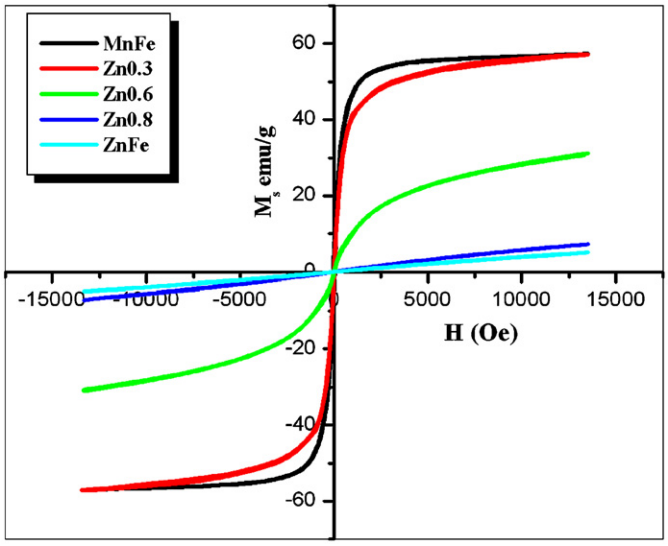

Fig. 7. Hysteresis curves at 300 K.

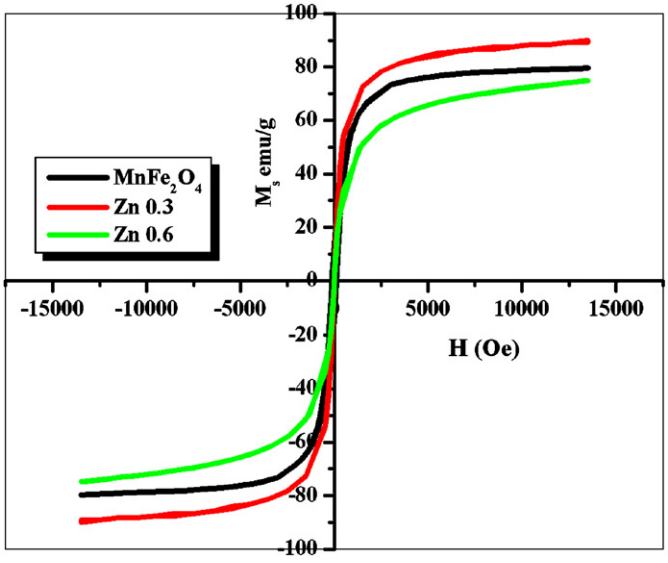

Fig. 8. Hysteresis curves at 100 K.

affects the T_c. The anomalous features observed in the compositions for $x \geqslant 0.5$ is unique and interesting.

The specific magnetization σ_s of the different compositions at 0 K are estimated by extrapolating the M–T graph to the Y-axis at 0 K. Magnetic moment in units of Bohr magnetons n_B (Table 2), can be calculated as [24]

$$n_B = \frac{\text{Mol. wt} \times \sigma_s}{5585}$$

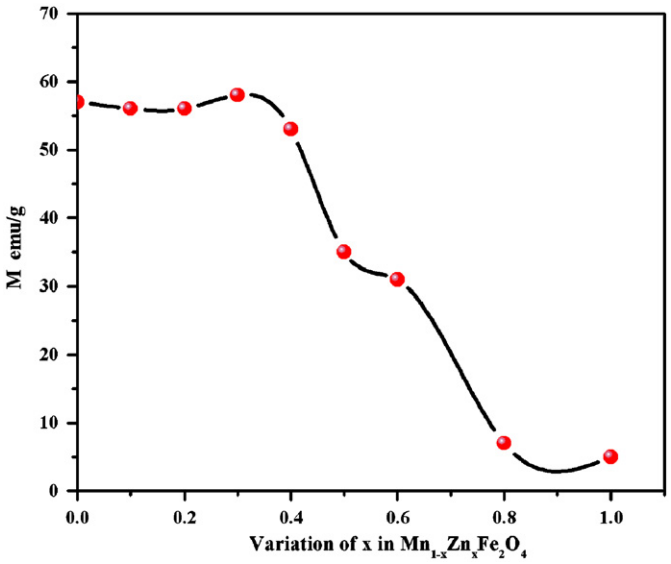

Fig. 9. Variation of magnetization with zinc.

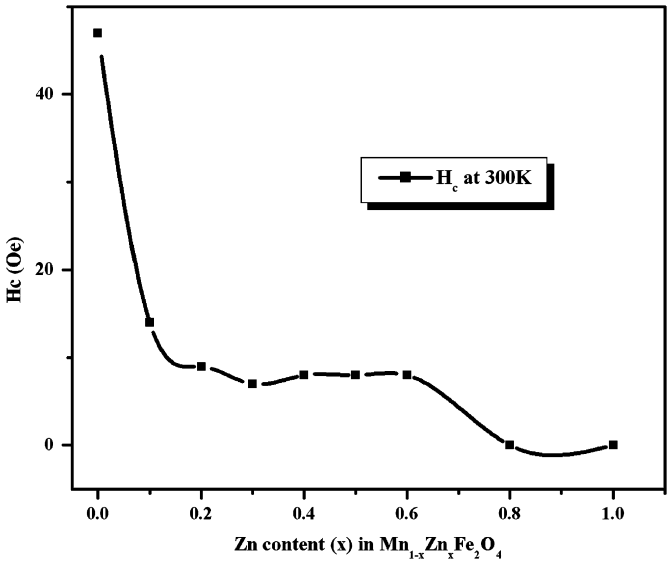

Fig. 10. Variation of H_c values with zinc.

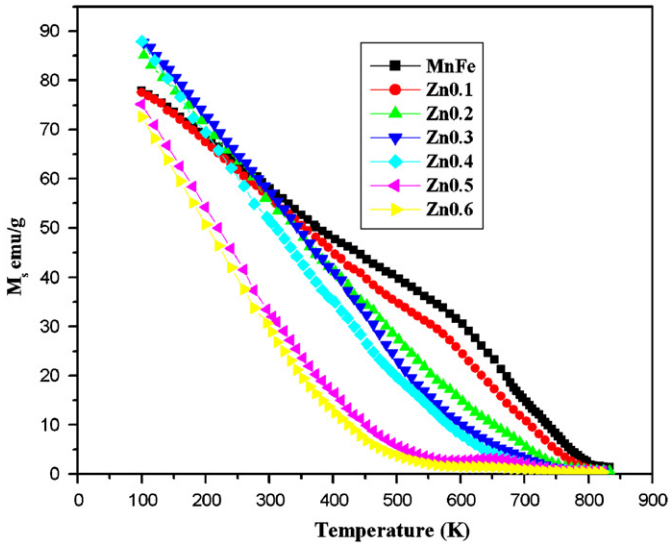

Fig. 11. M–T curves of $Mn_{1-x}Zn_xFe_2O_4$.

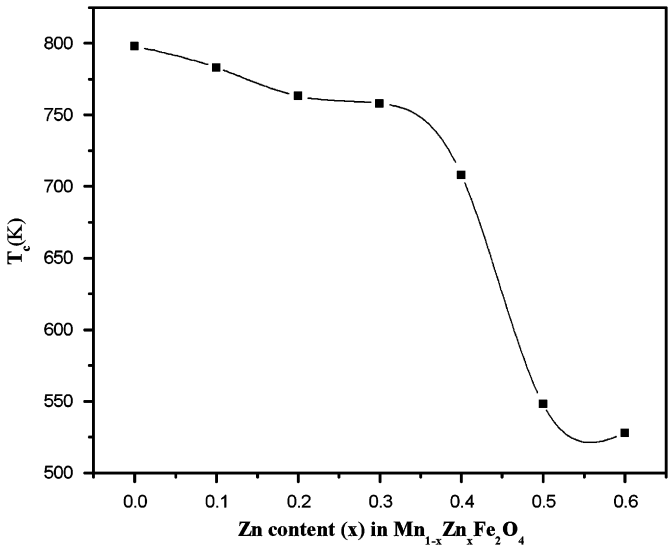

Fig. 12. Variation of T_c with zinc content.

where n_B is the magnetic moment (number of Bohr magnetons) and σ_s is the saturation magnetization per gram at 0 K.

The calculated values were found to be lower than the values of their corresponding cousins in the bulk [16] (Table 2). For manganese ferrite nanoparticles the calculated magnetic moment was 3.67 μ_B (4.6 μ_B for bulk). Based on the calculated μ_B from magetisation values a tentative cation distribution is formulated and is as follows: $Mn_{0.3323}Fe_{0.6677}[Mn_{0.6597}Fe_{1.3403}]$. This is based on the Neel's two sublattice [25] model and Chikazumi's approach [8]. Here it is assumed that the cation distribution is only responsible for the decrease in magnetization and other phenomena like surface effects, formation of dead layer, finite size effects are not taken into account. The inversion factor is calculated to be 66.5%. The presence of Mn^{3+} is also clearly evident in the cation distribution. While an inversion of 20% was observed in bulk samples [8], an inversion of 66.5% was obtained in our nanosized manganese ferrite. This inversion factor was found to be consistent with the reported values. However a detailed investigation employing Mossbauer spectroscopy, neutron diffraction and EXAFS is necessary to arrive at the exact cation distribution for the other compositions.

Both structural and magnetic characterization provide sufficient evidence for the existence of a metastable cation distribution at the nanoregime. Enhancement of T_c values together with lower magnetization and coercivity values of the series were found to depend on zinc substitution directly. Consequently by varying only the zinc concentration ratio we can tune the compositions with required structural and magnetic properties for various applications.

4. Conclusions

Nanocrystalline manganese zinc ferrite particles $Mn_{1-x}Zn_xFe_2O_4$ for $x = 0$ to 1 were prepared using the wet chemical co-precipitation technique. The particles were found to be exhibiting a spinel structure with sizes varying from 7 to 29 nm. The decrease in particle size and the lattice contraction with increasing zinc concentration in the nanoparticles were due to the occurrence of a metastable cation distribution different from their bulk counterpart. The compositional analysis confirmed the stiochiometry of the samples. The deviations in the case of magnetization with zinc concentration along with the lower magnetization values compared with the bulk are additional evidences for the existence of the metastable cation distribution. Enhanced T_c values obtained are indicative of a non-equilibrium cation distribution in the different compositions. The magnetic moment at zero Kelvin was estimated from the temperature dependence of magnetization and a tentative cation distribution for manganese ferrite is proposed. The presence of Mn^{3+}, an inversion of 66.5% and deviation in cation distribution was evident in the proposed cation distribution.

Acknowledgements

EVG acknowledges the Cochin University of Science and Technology for the Research Fellowship. KAM thanks University Grant Commission, Government of India for the financial assistance received under UGC minor project. Al-Omari would like to thank the Sultan Qaboos University for the support under Grant no. IG-SCI-PHYS-07-05. MRA acknowledges AICTE, Government of India ('Centre for ferrofluids' File no. 8023/RID/ RPS-73/ 2004-05, dated 29/03/2005) for the financial assistance.

References

[1] S. Sun, C.B. Murray, D. Weller, L. Folks, A. Moser, Science 287 (2000) 1989.
[2] Q.A. Pankhurst, J. Connolly, S.K. Jones, J. Dobson, J. Phys. D: Appl. Phys. 36 (2003) R167.
[3] S.D. Shenoy, P.A. Joy, M.R. Anantharaman, J. Magn. Magn. Mater. 269 (2004) 217.
[4] M.R. Anantharaman, S. jagadeeshan, K.A. Malini, S. Sindhu, A. Narayanasswamy, C.N. Chinnasamy, J.P. Jacobs, S. Rejine, K. Sheshan, R.H.H. Smits, H.H. Brongersma, J. Magn. Magn. Mater. 189 (1998) 83.
[5] F.K. Lotgering, J. Phys. Chem. Solids 27 (1996) 139.
[6] C.N. Chinnasamy, A. Narayanaswamy, N. Ponpandian, K. Chattopadhyay, K. Shinoda, B. Jeyadevan, K. Tohji, K. Nakatsuka, T. Furubayashi, I. Nakatani, Phys. Rev. B 63 (2001) 184108.
[7] A.H. Morrish, K. Haneeda, J. Appl. Phys. 52 (1981) 2496.
[8] Soshin Chikazumi, Physics of Ferromagnetism, Clarendon Press, Oxford, 1997, pp. 200–203.
[9] J. Sakurai, T. Shinjo, J. Phys. Soc. Jpn. 23 (1967) 1426.
[10] C. Rath, N.C. Mishra, S. Anand, R.P. Das, K.K. Sahu, C. Upadhyay, H.C. Verma, Appl. Phys. Lett. 76 (2000) 475.
[11] R. Arulmurugan, B. Jayadevan, G. Vaidyanathan, S. Sendhilnathan, J. Magn. Magn. Mater. 288 (2005) 470.
[12] C. Rath, K.K. Sahoo, S. Anand, S.K. Date, N.C. Mishra, R.P. Das, J. Magn. Magn. Mater. 202 (1999) 77.
[13] K. Majima, M. Hasegawa, S. Katsuyama, H. Nagai, S. Mishima, J. Mater. Sci. Lett. 12 (1993) 185.

[14] Mellisa A. Denecke, W. Gun Ber, G. Buxbaum, P. Kuske, Mater. Res. Bull. 27 (1992) 507.
[15] K.J. Standley, Oxide Magnetic Materials, Clarendon Press, Oxford, 1972.
[16] D.J. Craik, Magnetic Oxides, Part 1, Wiley, New York, 1975.
[17] J.M.D. Coey, Phys. Rev. Lett. 27 (1971) 1140.
[18] M. Garcia del Muro, X. Batlle, A. Labarta, Phys. Rev. B 59 (1999) 13584.
[19] Z.X. Tang, J.P. Chen, C.M. Sorenson, K.J. Klabunde, G.C. Hadjipanayis, Phys. Rev. Lett. 68 (1992) 3114.
[20] P.V. Hendriksen, S. Linderoth, P.A. Lindgard, Phys. Rev. B 48 (1993) 7259.
[21] N.S. Gajbhiye, Met. Mater. Process. 10 (1998) 247.
[22] W. Wolski, E. Wolska, J. Kaczmarek, P. Piszora, Phys. Status Solidi A 152 (1995) K19.
[23] C. Rath, N.C. Mishra, S. Anand, S.K. Date, R.P. Das, S.D. Kulkarni, K.K. Sahu, J. Appl. Phys. 91 (2002) 2211.
[24] J. Smit, H.P.J. Wijn, Ferrites, Philips Technical Library, Eindhoven, Netherlands, 1959.
[25] L. Neel, Ann. Phys. 12 (1948) 137.